Human knockouts in a cohort with a high rate of consanguinity

Danish Saleheen[1,2]†*, Pradeep Natarajan[3,4]†, Wei Zhao[1], Asif Rasheed[2], Sumeet Khetarpal[5], Hong-Hee Won[3,4], Konrad J. Karczewski[4,6], Anne H. O'Donnell-Luria[4,6,7], Kaitlin E. Samocha[6], Namrata Gupta[4], Mozzam Zaidi[2], Maria Samuel[2], Atif Imran[2], Shahid Abbas[8], Faisal Majeed[2], Madiha Ishaq[2], Saba Akhtar[2], Kevin Trindade[5], Megan Mucksavage[5], Nadeem Qamar[9], Khan Shah Zaman[9], Zia Yaqoob[9], Tahir Saghir[9], Syed Nadeem Hasan Rizvi[9], Anis Memon[9], Nadeem Hayyat Mallick[10], Mohammad Ishaq[11], Syed Zahed Rasheed[11], Fazal-ur-Rehman Memon[12], Khalid Mahmood[13], Naveeduddin Ahmed[14], Ron Do[15,16], Daniel G. MacArthur[4,6], Stacey Gabriel[4], Eric S. Lander[4], Mark J. Daly[4,6], Philippe Frossard[2]†, John Danesh[17,18]†, Daniel J. Rader[5,19]†, Sekar Kathiresan[3,4]†*

†Contributed equally

[1] Department of Biostatistics and Epidemiology, Perelman School of Medicine at the University of Pennsylvania, Philadelphia, PA, USA

[2] Center for Non-Communicable Diseases, Karachi, Pakistan

[3] Center for Human Genetic Research and Cardiovascular Research Center, Massachusetts General Hospital, Boston, MA, USA

[4] Broad Institute of Harvard and MIT, Cambridge, MA, USA

[5] Division of Translational Medicine and Human Genetics, Department of Medicine, Perelman School of Medicine at the University of Pennsylvania, Philadelphia, PA, USA

[6] Analytic and Translational Genetics Unit, Department of Medicine, Massachusetts General Hospital and Harvard Medical School, Boston, MA

[7] Division of Genetics and Genomics, Boston Children's Hospital, Boston, MA, USA

[8] Faisalabad Institute of Cardiology, Faisalabad, Pakistan

[9] National Institute of Cardiovascular Disorders, Karachi, Pakistan

[10] Punjab Institute of Cardiology, Lahore, Pakistan

[11] Karachi Institute of Heart Diseases, Karachi, Pakistan

[12] Red Crescent Institute of Cardiology, Hyderabad, Pakistan

[13] The Civil Hospital, Karachi, Pakistan

[14] Liaquat National Hospital, Karachi, Pakistan

[15] Department of Genetics and Genomic Sciences, Mount Sinai Medical Center, Icahn School of Medicine at Mount Sinai, New York, NY, USA

[16] The Charles Bronfman Institute of Personalized Medicine, Icahn School of Medicine at Mount Sinai, New York, NY, USA

[17] Department of Public Health and Primary Care, University of Cambridge, UK

[18] Wellcome Trust Sanger Institute, Hinxton, Cambridge, UK

[19] Department of Human Genetics, University of Pennsylvania, USA

*Corresponding authors:

Danish Saleheen, MBBS, PhD

Department of Biostatistics and Epidemiology

University of Pennsylvania

11-134 Translational Research Center

3400 Civic Center Boulevard

Philadelphia, PA 19104

Tel: 215-573-6323

Fax: 215-573-2094

Email: saleheen@mail.med.upenn.edu

Sekar Kathiresan, MD

Broad Institute and Massachusetts General Hospital

CPZN 5.252

185 Cambridge Street

Boston, MA 02114

Tel: 617-643-6120

Email: sekar@broadinstitute.org

Word Count, Summary Paragraph: 253

Word Count, Main Text: 1,977

Summary Paragraph

A major goal of biomedicine is to understand the function of every gene in the human genome.[1] Null mutations can disrupt both copies of a given gene in humans and phenotypic analysis of such 'human knockouts' can provide insight into gene function. To date, comprehensive analysis of genes knocked out in humans has been limited by the fact that null mutations are infrequent in the general population and so, observing an individual homozygous null for a given gene is exceedingly rare.[2,3] However, consanguineous unions are more likely to result in offspring who carry homozygous null mutations. In Pakistan, consanguinity rates are notably high.[4] Here, we sequenced the protein-coding regions of 7,078 adult participants living in Pakistan and performed phenotypic analysis to identify homozygous null individuals and to understand consequences of complete gene disruption in humans. We enumerated 36,850 rare (<1 % minor allele frequency) null mutations. These homozygous null mutations led to complete inactivation of 961 genes in at least one participant. Homozygosity for null mutations at *APOC3* was associated with absent plasma apolipoprotein C-III levels; at *PLAG27*, with absent enzymatic activity of soluble lipoprotein-associated phospholipase A2; at *CYP2F1*, with higher plasma interleukin-8 concentrations; and at either *A3GALT2* or *NRG4*, with markedly reduced plasma insulin C-peptide concentrations. After physiologic challenge with oral fat, *APOC3* knockouts displayed marked blunting of the usual post-prandial rise in plasma triglycerides compared to wild-type family members. These observations provide a roadmap to understand the consequences of complete disruption of a large fraction of genes in the human genome.

85 **Main Text**

86 We studied adult participants in the Pakistan Risk of Myocardial Infarction Study
87 (PROMIS) designed to understand the determinants of cardiometabolic diseases in South
88 Asians.[5] Consanguineous marriages have been common in this region of South Asia for
89 many generations.[6] In PROMIS, 38.3% of participants reported that their parents were
90 cousins and 38.1% reported themselves being married to a cousin. An expectation from
91 consanguinity is long regions of autozygosity, defined as homozygous loci identical by
92 descent.[7] Using genome-wide genotyping data available in 17,744 PROMIS participants,
93 we quantified the length of runs of homozygosity, defined as homozygous segments at
94 least 1.5 megabases long. We compared the lengths of runs of homozygosity among
95 PROMIS participants with that seen in other populations from the International HapMap3
96 project. Median length of genome-wide homozygosity among PROMIS participants was
97 6-7 times higher than participants of European (CEU, TSI) ($P = 3.6 \times 10^{-37}$), East Asian
98 (CHB, JPT, CHD) ($P = 5.4 \times 10^{-48}$) and African ancestries (YRI, MKK) ($P = 1.3 \times 10^{-40}$),
99 respectively (**Fig. 1**).

100 In order to characterize the burden of rare homozygous null alleles, we performed
101 whole exome sequencing in 7,078 PROMIS participants (**Table 1**). Across all
102 participants, 1,303,689 protein-coding and splice-site sequence variants in 20,008
103 autosomal genes passed variant quality control metrics. Of these, 47,656 mutations across
104 13,645 autosomal genes were annotated as null (nonsense, frameshift, or canonical
105 splice-site). To increase the probability that mutations annotated as null are *bona fide*, we
106 removed nonsense and frameshift mutations occurring within the last 5% of the transcript
107 and within exons flanked by non-canonical splice sites, splice site mutations at small

(<15 bp) introns, at non-canonical splice sites, and where the purported null allele is observed across primates. Common null alleles are less likely to exert strong functional effects as they are less constrained by purifying selection; thus, we limit our analyses in the rest of the manuscript to null mutations with a minor allele frequency (MAF) of < 1%.

Applying these criteria, we generated a set of 36,850 null mutations across 12,131 autosomal genes.[8] The site-frequency spectrum for these null mutations revealed that the majority was seen only in one or a few individuals (**Fig. 2**).

We compared the coefficient of inbreeding (F coefficient) in PROMIS participants with that of 15,249 individuals from outbred populations of European or African American ancestry. The F coefficient estimates the excess homozygosity compared with an estimated outbred ancestor. PROMIS participants had a 4-fold higher median inbreeding coefficient compared to outbred populations (0.016 v 0.0041; $P < 2 \times 10^{-16}$) (**Fig. 3A**). Additionally, those in PROMIS who reported that their parents were closely related had even higher median inbreeding coefficients than those who did not (0.024 v 0.013; $P < 2 \times 10^{-16}$).

Across all 7,078 PROMIS participants, both copies of 961 distinct genes were disrupted due to null mutations with MAF < 1%. A full listing of all 961 genes knocked out, the number of knockout participants for each gene, and the specific null mutation(s) are provided in **Supplementary Table 1**. 697 (72.5 %) of the genes were knocked out only in one participant (**Supplementary Figure 1**). About 1 in 5 sequenced participants (1,306 individuals, 18.4 %) had at least one gene knocked by a homozygous null mutation with MAF < 1%. 1,081 of these 1,306 individuals (82.8 %) had complete

deficiency for one gene, but a minority of participants were knockouts for more than one gene and one participant had six genes completely inactivated. The F inbreeding coefficient was correlated with the number of homozygous null genes present in each individual. (Spearman r = 0.29; $P = 3 \times 10^{-133}$) (**Fig. 3B**).

We tested the hypothesis that genes observed in the homozygous null state in PROMIS participants are under less evolutionary constraint. We calculated the probability of being loss-of-function intolerant (at >90% threshold) for each gene (see Methods) [9,10] and. compared this to 961 randomly selected genes. The observed 961 homozygous null genes were less likely to be classified as highly constrained (odds ratio 0.10; 95% CI 0.095, 0.11; $P < 1 \times 10^{-10}$).

We next sought to understand the phenotypic consequences of complete disruption of any of these 961 genes. We applied two approaches. First, for 264 genes where two or more participants were homozygous null, we conducted an association screen against a panel of 201 phenotypic traits (**Supplementary Table 2**). Second, at a single gene, we recalled participants based on genotype across three classes ('wild-type', heterozygous null, and homozygous null) and performed provocative physiologic testing.

At 264 genes where two or more participants were homozygous null, we performed association analyses to determine whether homozygous null mutation status was associated with variation in any of 201 traits. For quantitative traits, we compared mean trait values in homozygous null carriers with non-carriers. For dichotomous traits, we performed logistic regression with trait status as the outcome variable and homozygous null carrier status as the predictor variable. Details of covariate adjustments are presented in the Methods. Across quantitative and dichotomous traits, this resulted in

the analysis of 15,263 gene-trait pairs and thus, we set Bonferroni-adjusted significance threshold at $P = 3 \times 10^{-6}$.

The quantile-quantile plot of expected versus observed association results shows an excess of highly significant results without systematic inflation (**Supplementary Figure 2**). Association results surpassed the Bonferroni significance threshold for 14 gene-trait pairs (**Supplementary Table 3**). Below, we highlight four associations demonstrating examples of 1) confirmed biochemical deficiency with two independent assays (*PLA2G7*), 2) gene-biomarker association (*CYP2F1*), 3) pure recessive model of association (*A3GALT2*), and 4) confirmed biochemical deficiency with gene-biomarker association (*APOC3*).

Lipoprotein-associated phospholipase A2 (Lp-PLA2, encoded by *PLA2G7*) hydrolyzes oxidatively-modified polyunsaturated fatty acids producing lysophosphatidylcholine and oxidized nonesterified fatty acids. Higher soluble Lp-PLA2 activity has been correlated with higher risk for cardiovascular disease.[11] At *PLA2G7*, we identified two participants homozygous for *PLA2G7* c.663+1G>A. When compared with non-carriers, c.663+1G>A homozygotes have markedly lower Lp-PLA2 enzyme as well as activity (-266 ng/ml, $P = 7 \times 10^{-5}$ for mass; -245 nmol/ml/min, $P = 2 \times 10^{-7}$ for activity) whereas the 102 heterozygotes had an intermediate effect (-107 ng/ml, $P = 4 \times 10^{-26}$ for mass; -115 nmol/ml/min, $P = 3 \times 10^{-58}$ for activity) (**Supplementary Figure 3a-b**).

Cytochrome P450 2F1 (encoded by *CYP2F1*) is primarily expressed in the lung and metabolizes pulmonary-selective toxins, such as cigarette smoke, and thus, modulates the expression of environmentally-associated pulmonary diseases.[12] At

177 *CYP2F1*, we identified two participants homozygous for a splice-site mutation, c.1295-
178 2A>G. When compared with non-carriers, c.1295-2A>G homozygotes displayed higher
179 soluble interleukin 8 concentrations (+40.3 %; $P = 3 \times 10^{-6}$) (**Supplementary Figure 4**).
180 *CYP2F1* c.1295-2A>G heterozygotes (n = 3 assayed for interleukin 8) had a more modest
181 effect (+10.7 %; $P = 2 \times 10^{-4}$). Interleukin 8 is a mediator of acute pulmonary
182 inflammation.[13]

183 Alpha-1,3-galactosyltransferase 2 (encoded by *A3GALT2*) catalyzes the formation
184 of the Gal-α1-3Galβ1-4GlcNAc-R (α-gal) epitope; the biological role of this enzyme in
185 humans is uncertain.[14] At *A3GALT2*, we identified two participants homozygous for a
186 frameshift mutation, p.Thr106SerfsTer4. Compared with non-carriers, p.Thr106SerfsTer4
187 homozygotes had both reduced fasting insulin C-peptide (-97.4%; $P = 6 \times 10^{-12}$) as well
188 as total fasting insulin concentrations (-91.9%; $P = 1 \times 10^{-4}$). Such an association was
189 only observed in the homozygous state (**Supplementary Figure 5**). *A3galt2*$^{-/-}$ mice and
190 pigs have recently been shown to have glucose intolerance.[15,16]

191 To understand if the identification of only a single homozygote in PROMIS may
192 still be informative, we performed a complementary analysis, focusing on those with the
193 most extreme standard Z scores (|Z score| > 5) and requiring that there be evidence for
194 association in heterozygotes as well (see Methods). This procedure highlighted neureglin
195 4 (NRG4), a member of the epidermal growth factor family extracellular ligands which is
196 highly expressed in brown fat, particularly during adipocyte differentiation.[17,18] At *NRG4*,
197 we identified a single participant homozygous for a frameshift mutation,
198 p.Ile75AsnfsTer23, who had nearly absent fasting insulin C-peptide concentrations (-99.3
199 %; $P = 7 \times 10^{-11}$). When compared with non-carriers, heterozygotes for *NRG4*

p.Ile75AsnfsTer23 (n = 7) displayed 54.5 % reduction in insulin C-peptide ($P = 6 \times 10^{-3}$). Mice homozygous deleted for *Nrg4* have recently been shown to have glucose intolerance.[18]

Apolipoprotein C-III (apoC-III, encoded by *APOC3*) is a major protein component of chylomicrons, very low-density lipoprotein cholesterol, and high-density lipoprotein cholesterol.[19] We and others recently reported that null mutations in heterozygous form lower plasma triglycerides as well as risk for coronary heart disease.[20,21] In both published studies, no *APOC3* homozygotes were identified despite study of nearly 200,000 participants from the U.S. and Europe. However, in this study of about 7,000 Pakistanis, we identified four participants homozygous for *APOC3* p.Arg19Ter. When compared with non-carriers, p.Arg19Ter homozygotes displayed near-absent plasma apoC-III protein (-89.4 %, $P = 5 \times 10^{-24}$), lower plasma triglyceride concentrations (-61.7 %, $P = 4 \times 10^{-4}$), higher high-density lipoprotein (HDL) cholesterol (+28.1 mg/dL, $P = 6 \times 10^{-9}$); and similar levels of low-density lipoprotein (LDL) cholesterol ($P = 0.11$) (**Fig. 4a-d**).

ApoC-III functions as a brake on the metabolism of dietary fat and thus, the complete lack of this protein should promote handling of ingested fat. The availability of humans completely deficient in APOC3 allowed us to test this hypothesis directly. We re-contacted one homozygous null proband, his wife, and 27 of his first-degree relatives for genotyping and physiologic investigation. Surprisingly, we found that the proband's wife was also a null homozygote, leading to all nine children being obligate homozygotes (**Fig. 4e**). In this family, we challenged homozygotes (n = 6) and non-carriers (n = 7) with a 50 g/m^2 oral fat load followed by serial blood testing for six hours. *APOC3* p.Arg19Ter

223 carriers had significantly lower post-prandial triglyceride excursions (triglycerides area
224 under the curve 468.3 mg/dL*6 hours vs 1267.7 mg/dL*6 hours; $P = 1 \times 10^{-4}$) (**Fig. 4f**).
225 These data show that complete lack of APOC3 markedly improves clearance of plasma
226 triglycerides after a fatty meal.

227 Gene disruption in model organisms followed by phenotypic analysis has been a
228 fruitful approach to understand gene function; here, we extend this concept to the human
229 organism, leveraging naturally-occurring null mutations, consanguinity, and extensive
230 biochemical phenotyping. These results permit several conclusions.

231 First, power to identify human knockouts is improved with the study of
232 populations with high degrees of consanguinity. Using the observed median inbreeding
233 coefficient of sequenced participants, we estimate that with the sequencing of 200,000
234 Pakistanis, about 8,754 genes (95% CI, 8,669-8,834) will be completely knocked out in at
235 least one participant (**Fig. 5**). In contrast, with the sequencing of a similar number of
236 outbred individuals of European, East Asian, or African American ancestries, the
237 expected number of genes knocked out is much less at 1,382 (95% CI, 1,339-1,452),
238 1,423 (95% CI, 1,388-1,457), and 1,822 (95% CI, 1,772-1,871), respectively (minor
239 allele frequency estimates obtained from the Exome Aggregation Consortium, manuscript
240 submitted in parallel). Thus, if a similar number of individuals were sequenced across
241 different ancestries, the number of genes completely knocked out would be nearly six-
242 fold higher in Pakistanis when compared with other outbred populations. For example,
243 among >100,000 participants in Iceland, 1107 homozygous null genes were identified
244 whereas we observe nearly the same number of null genes after analysis of about 7,000
245 Pakistanis.[3]

Second, dense phenotyping can uncover a range of phenotypic consequences from complete disruption of a gene as observed for *PLA2G7*, *CYP2F1*, *A3GALT2* and *NRG4*. Third, recall of complete human knockouts followed by provocative testing may provide physiologic insights. We used this approach to demonstrate that complete lack of apolipoprotein C-III is tolerated and results in both lowered fasting triglyceride concentrations as well as blunted post-prandial lipemia. Finally, to date, most human genetic studies have pursued a phenotype-first ("forward" genetics) approach, beginning with traits of interest followed by genetic mapping. Here, we show that it is now possible to pursue a systematic genotype-first ("reverse" genetics) approach, starting with homozygous null humans followed by methodical examination of a diverse set of traits.

Methods

General overview of the Pakistan Risk for Myocardial Infarction Study (PROMIS).

The PROMIS study is designed to investigate determinants of cardiometabolic diseases in Pakistan. Since 2005, the study has enrolled close to 38,000 participants; the present investigation included 7,078 participants. Participants aged 30-80 years were enrolled from nine recruitment centers based in five major urban cities in Pakistan. Type 2 diabetes in the study was defined based on self-report or fasting glucose levels >125 mg/dL or HbA1c > 6.5 % or use of glucose lowering medications. The study was approved by the institutional review board at the Center for Non-Communicable Diseases (IRB: 00007048, IORG0005843, FWAS00014490) and all participants gave informed consent.

Phenotype descriptions.

Non-fasting blood samples (with the time since last meal recorded) were drawn and centrifuged within 45 minutes of venipuncture. Serum, plasma and whole blood samples were stored at -70°C within 45 minutes of venipuncture. All samples were transported on dry ice to the central laboratory at the Center for Non-Communicable Diseases (CNCD), Pakistan, where serum and plasma samples were aliquoted across 10 different storage vials. Samples were stored at -70°C for any subsequent laboratory analyses. All biochemical assays were conducted in automated auto-analyzers. At CNCD Pakistan, measurements for total-cholesterol, HDL cholesterol, LDL cholesterol, triglycerides, and creatinine were made in serum samples using enzymatic assays; whereas levels of HbA1c were measured using a turbidemetric assay in whole-blood samples (Roche Diagnostics,

USA). For further measurements, aliquots of serum and plasma samples were transported on dry ice to the Smilow Research Center, University of Pennsylvania, USA, where following biochemical assays were conducted: apolipoproteins (apoA-I, apoA-II, apoB, apoC-III, apoE) and non-esterified fatty acids were measured through immunoturbidometric assays using kits by Roche Diagnostics or Kamiya; lipoprotein (a) levels were determined through a turbidimetric assay using reagents and calibrators from Denka Seiken (Niigata, Japan); LpPLA2 mass and activity levels were determined using immunoassays manufactured by diaDexus (San Francisco, CA, USA); measurements for insulin, leptin and adiponectin were made using radio-immunoassays by LINCO (MO, USA); levels of adhesion molecules (ICAM-1, VCAM-1, P- and E-Selectin) were determined through enzymatic assays by R&D (Minneapolis, MN, USA); and measurements for C-reactive protein, alanine transaminase, aspartate transaminase, cystatin-C, ferritin, ceruloplasmin, thyroid stimulating hormone, alkaline phosphatase, sodium, potassium, choloride, phosphate, sex-harmone binding globulin were made using enzymatic assays manufactured by Abbott Diagnostics (NJ, USA). Glomerular filtration rate (eGFR) was estimated from serum creatinine levels using the MDRD equation. ApoC-III levels were determined in an autoanalyzer using a commercially available ELISA by Sekisui Diagnostics (Lexington, USA). We also measured the following 52 protein biomarkers by multiplex immunoassay using a customised panel on the Luminex 100/200 instrument by RBM (Myriad Rules Based Medicine, Austin, TX, USA): fatty acid binding protein, granuloctye monocyte colony stimulating factor, granulocyte colony stimulating factor, interferon gamma, interleukin-1 beta, interleukin 1 receptor, interleukin 2, interleukin 3, interleukin 4, interleukin 5, interleukin 6, interleukin 7,

303 interleukin 8, interleukin 10, interleukin 18, interleukin p40, interleukin p70, interleukin
304 15, interleukin 17, interleukin 23, macrophage inflammatory protein 1 alpha, macrophage
305 inflammatory protein 1 beta, malondialdehyde-modified LDL, matrix metalloproteinase
306 2, matrix metalloproteinase 3, matrix metalloproteinase 9, nerve growth factor beta,
307 tumor necrosis factor alpha, tumor necrosis factor beta, brain-derived neurotrophic factor,
308 CD40, CD40 ligand, eotaxin, factor VII, insulin-like growth factor 1, lecithin-type
309 oxidized LDL receptor 1, monocyte chemoattractant protein 1, myeloperoxidase, N-
310 terminal prohormone of brain natriuretic peptide, neuronal cell adhesion molecule,
311 pregnancy-associated plasma protein A, soluble receptor for advanced glycation end-
312 products, sortilin, stem cell factor, stromal cell-derived factor 1, thrombomodulin, S100
313 calcium binding protein B, and vascular endothelial growth factor.
314
315 **Laboratory methods for array-based genotyping.**
316 As previously described, a genomewide association scan was performed using the
317 Illumina 660 Quad array at the Wellcome Trust Sanger Institute (Hinxton, UK) and using
318 the Illumina HumanOmniExpress at Cambridge Genome Services, UK.[22] Initial quality
319 control (QC) criteria included removal of participants or single nucleotide
320 polymorphisms (SNPs) that had a missing rate >5%. SNPs with a MAF <1% and a P-
321 value of $<10^{-7}$ for the Hardy-Weinberg equilibrium test were also excluded from the
322 analyses. In PROMIS, further QC included removal of participants with discrepancy
323 between their reported sex and genetic sex determined from the X chromosome. To
324 identify sample duplications, unintentional use of related samples (cryptic relatedness)

and sample contamination (individuals who seem to be related to nearly everyone in the sample), identity-by-descent (IBD) analyses were conducted in PLINK.[23]

Laboratory methods for exome sequencing.

Exome sequencing. Exome sequencing was performed at the Broad Institute. Sequencing and exome capture methods have been previously described.[24,25] A brief description of the methods is provided below.

Receipt/quality control of sample DNA. Samples were shipped to the Biological Samples Platform laboratory at the Broad Institute of MIT and Harvard (Cambridge, MA, USA). DNA concentration was determined by PicoGreen (Invitrogen; Carlsbad, CA, USA) prior to storage in 2D-barcoded 0.75 ml Matrix tubes at -20 ^{o}C in the SmaRTStore (RTS, Manchester, UK) automated sample handling system. Initial quality control (QC) on all samples involving sample quantification (PicoGreen), confirmation of high-molecular weight DNA and fingerprint genotyping and gender determination (Illumina iSelect; Illumina; San Diego, CA, USA). Samples were excluded if the total mass, concentration, integrity of DNA or quality of preliminary genotyping data was too low.

Library construction. Library construction was performed as previously described[26], with the following modifications: initial genomic DNA input into shearing was reduced from 3µg to 10-100ng in 50µL of solution. For adapter ligation, Illumina paired end adapters were replaced with palindromic forked adapters, purchased from Integrated DNA Technologies, with unique 8 base molecular barcode sequences included in the adapter sequence to facilitate downstream pooling. With the exception of the palindromic forked adapters, the reagents used for end repair, A-base addition, adapter ligation, and

348 library enrichment PCR were purchased from KAPA Biosciences (Wilmington, MA,
349 USA) in 96-reaction kits. In addition, during the post-enrichment SPRI cleanup, elution
350 volume was reduced to 20 µL to maximize library concentration, and a vortexing step
351 was added to maximize the amount of template eluted.
352 **In-solution hybrid selection.** 1,973 samples underwent in-solution hybrid selection as
353 previously described[26], with the following exception: prior to hybridization, two
354 normalized libraries were pooled together, yielding the same total volume and
355 concentration specified in the publication. 5,263 samples underwent hybridization and
356 capture using the relevant components of Illumina's Rapid Capture Exome Kit and
357 following the manufacturer's suggested protocol, with the following exceptions: first, all
358 libraries within a library construction plate were pooled prior to hybridization, and
359 second, the Midi plate from Illumina's Rapid Capture Exome Kit was replaced with a
360 skirted PCR plate to facilitate automation. All hybridization and capture steps were
361 automated on the Agilent Bravo liquid handling system.
362 **Preparation of libraries for cluster amplification and sequencing.** Following post-
363 capture enrichment, libraries were quantified using quantitative PCR (KAPA Biosystems)
364 with probes specific to the ends of the adapters. This assay was automated using
365 Agilent's Bravo liquid handling platform. Based on qPCR quantification, libraries were
366 normalized to 2nM and pooled by equal volume using the Hamilton Starlet. Pools were
367 then denatured using 0.1 N NaOH. Finally, denatured samples were diluted into strip
368 tubes using the Hamilton Starlet.
369 **Cluster amplification and sequencing.** Cluster amplification of denatured templates
370 was performed according to the manufacturer's protocol (Illumina) using HiSeq v3

371 cluster chemistry and HiSeq 2000 or 2500 flowcells. Flowcells were sequenced on HiSeq
372 2000 or 2500 using v3 Sequencing-by-Synthesis chemistry, then analyzed using RTA
373 v.1.12.4.2. Each pool of whole exome libraries was run on paired 76bp runs, with and 8
374 base index sequencing read was performed to read molecular indices, across the number
375 of lanes needed to meet coverage for all libraries in the pool.
376 **Read mapping and variant discovery**. Samples were processed from real-time base-
377 calls (RTA v.1.12.4.2 software [Bustard], converted to qseq.txt files, and aligned to a
378 human reference (hg19) using Burrows–Wheeler Aligner (BWA).[27] Aligned reads
379 duplicating the start position of another read were flagged as duplicates and not analysed.
380 Data was processed using the Genome Analysis ToolKit (GATK v3).[28-30] Reads were
381 locally realigned around indels and their base qualities were recalibrated. Variant calling
382 was performed on both exomes and flanking 50 base pairs of intronic sequence across all
383 samples using the HaplotypeCaller (HC) tool from the GATK to generate a gVCF. Joint
384 genotyping was subsequently performed and 'raw' variant data for each sample was
385 formatted (variant call format (VCF)). SNVs and indel sites were initially filtered after
386 variant calibration marked sites of low quality that were likely false positives.
387 **Data analysis QC**. Fingerprint concordance between sequence data and fingerprint
388 genotypes was evaluated. Variant calls were evaluated on both bulk and per- sample
389 properties: novel and known variant counts, transition–transversion (TS–TV) ratio,
390 heterozygous–homozygous non-reference ratio, and deletion/insertion ratio. Both bulk
391 and sample metrics were compared to historical values for exome sequencing projects at
392 the Broad Institute. No significant deviation of from historical values was noted.
393

Data processing and quality control of exome sequencing.

Variant annotation. Variants were annotated using Variant Effect Predictor[31] and the LOFTEE[8] plugin to identify protein-truncating variants predicted to disrupt the respective gene's function with "high confidence." Each allele at polyallelic sites was separately annotated.

Sample level quality control. We performed quality control of samples using the following steps. For quality control of samples, we used bi-allelic SNVs that passed the GATK VQSR filter and were on genomic regions targeted by both ICE and Agilent exome captures. We removed samples with discordance rate > 10% between genotypes from exome sequencing with genotypes from array-based genotyping and samples with sex mismatch between inbreeding coefficient on chromosome X and fingerprinting. We tested for sample contamination using the verifyBamID software, which examines the proportion of non-reference bases at reference sites, and excluded samples with high estimated contamination (FREEMIX scores > 0.2).[32] After removing monozygotic twins or duplicate samples using the KING software[33], we removed outlier samples with too many or too few SNVs (>17,500 total variants for Agilent-captured samples or >18,000 for ICE-captured samples; <12,000 total variants; >600 singletons; and >400 doubletons). We removed those with extreme overall transition-to-transversion ratios (>4 or <3) and heterozygosity (heterozygote-to-homozygote ratio >6 or <2). Finally, we removed samples with high missingness (>0.05).

Variant level quality control. Variant score quality recalibration was performed separately for SNVs and indels use the GATK VariantRecalibrator and ApplyRecalibration to filter out variants with lower accuracy scores. To further reduce

the rate of inaccurate variant calls, we further filtered out SNVs with low average quality (quality per depth of coverage (QD) < 2) and a high degree of missingness (> 20 %), and indels also with low average quality (quality per depth of coverage (QD) < 3) and a high degree of missingness (> 20 %).

Methods for inbreeding analyses.

Array-derived runs of homozygosity. Analyses were conducted in PLINK[23] using genome-wide association (GWAS) data in PROMIS and HapMap 3 populations. Segments of the genome that were at-least 1.5 Mb long, had a SNP density of 1 SNP per 20 kb and had 25 consecutive homozygous SNPs (1 heterozygous and/or 5 missing SNPs were permitted within a segment) were defined to be in a homozygous state (or referred as "runs of homozygosity" (ROH)), as described previously.[34] Homozygosity was expressed as the percentage of the autosomal genome found in a homozygous state, and was calculated by dividing the sum of ROH length within each individual by the total length of the autosome in PROMIS and HapMap 3 populations respectively. To investigate variability in homozygosity explained by parental consanguinity, the difference in R^2 is reported for a linear regression model of homozygosity including and excluding parental consanguinity on top of age, sex and the first 10 principal components derived from the typed autosomal GWAS data.

Sequencing-derived coefficient of inbreeding. We compared the coefficient of inbreeding distributions of 7,078 exome sequenced PROMIS participants with 15,248 participants (European ancestry = 12,849, and African ancestry = 2,399) who were exome sequenced at the Broad Institute (Cambridge, MA) from the Myocardial Infarction

Genetics consortium.[25] We extracted approximately 5,000 high-quality polymorphic SNVs in linkage equilibrium present on both target intervals that passed variant quality control metrics based on HapMap 3 data.[35] Using PLINK, we estimated the coefficient of inbreeding separately within each ethnicity group.[23] The coefficient of inbreeding was estimated as the observed degree of homozygosity compared with the anticipated homozygosity derived from an estimated common ancestor.[36] The Wilcoxon-Mann-Whitney test was used to test whether PROMIS participants had different median coefficients of inbreeding compared to other similarly sequenced outbred individuals and whether the median coefficient of inbreeding was different between PROMIS participants who reported parental relatedness versus not. A two-sided *P* of 0.05 was the pre-specified threshold for statistical significance.

Methods for sequencing projection analysis.

To compare the burden of unique completely inactivated genes in the PROMIS cohort with outbred cohorts of diverse ethnicities, we extracted the minor allele frequencies (maf) of "high confidence" loss-of-function mutations observed in PROMIS, and in European, African, and East Asian ancestry participants from the Exome Aggregation Consortium (ExAC r0.3; exac.broadinstitute.org). For each gene and for each ethnicity, the combined minor allele frequency (cmaf) of rare (maf < 0.1%) “high confidence” loss-of-function mutations was calculated. We then simulated the number of unique completely inactivated genes across a range of sample sizes per ethnicity and PROMIS. The expected probability of observing complete inactivation (two null copies in an individual) of a gene was calculated as $(1 - F) * cmaf^{2} + F * cmaf$, which accounts

for allozygous and autozygous, respectively, mechanisms for complete genie knockout. F, the inbreeding coefficient, is defined as $F = 1 - (expected\ heterozygosity\ rate\ /\ observed\ heterozygosity\ rate)$. For PROMIS, the median F inbreeding coefficient (0.016) was used for estimation. Down-sampling within the observed sample size for both high-confidence null mutations and synonymous variants did not deviate significantly from the expected trajectory. For a range of sample sizes (0-200,000), each gene was randomly sampled under a binomial distribution ($X \sim B(n, cmaf)$) and it was determined if the gene was successfully sampled at least once. To refine the estimated count of unique genes per sample size, each sampling was replicated ten times.

Methods for constraint score analysis.

We sought to determine whether the observed homozygous null genes were under less evolutionary constraint by first obtaining constraint loss of function constraint scores derived from the Exome Aggregation Consortium (Lek M et al, in preparation).[9,10] Briefly, we used the number of observed and expected rare (MAF < 0.1%) loss of function variants per gene to determine to which of three classes it was likely to belong: null (observed variation matches expectation), recessive (observed variation is ~50% expectation), or haploinsufficient (observed variation is <10% of expectation). The probability of being loss of function intolerant (pLI) of each transcript was defined as the probability of that transcript falling into the haploinsufficient category. Transcripts with a pLI ≥ 0.9 are considered very likely to be loss of function intolerant; those with pLI ≤ 0.1 are not likely to be loss of function intolerant. A list of 961 genes were randomly sampled from a list of sequenced genes 1,000 times and the proportion of loss of function

intolerant genes compared to the proportion of the observed homozygous null genes was compared using the chi square test. The likelihood that the distribution of the test statistics deviated from the null was ascertained.

Methods for rare variant association analysis.

Recessive model association discovery. We sought to determine whether complete loss-of-function of a gene was associated with a dense array of phenotypes. We extracted a list of individuals per gene who were homozygous for a high confidence null allele that was rare (minor allele frequency < 1 %) in the cohort. From a list of 961 genes where there was at least one participant homozygous null and a list of 201 traits, we initially considered 192,960 gene-trait pairings. To reduce the likelihood of false positives, we only considered gene-trait pairs where there were at least two homozygous nulls per gene phenotyped for a given trait yielding 15,263 gene-trait pairs for analysis.

For all analyses, we constructed generalized linear models to test whether complete loss of function versus non-carriers was associated with trait variation. A logit link was used for binomial outcomes. Right-skewed continuous traits were natural log transformed. Age, sex, and myocardial infarction status were used as covariates in all analyses. We extracted principal components of ancestry using EIGENSTRAT to control for population stratification in all analyses.[37] For lipoprotein-related traits, the use of lipid-lowering therapy was used as a covariate. For glycemic biomarkers, only non-diabetics were used in the analysis. The *P* threshold for statistical significance was 0.05 / 15,263 = 3×10^{-6}.

Heterozygote association replication. We hypothesized that some of the associations for homozygous nulls will display a more modest effect for heterozygous nulls. Thus, the aforementioned analyses were performed comparing heterozygous nulls to non-carriers for the fourteen homozygous null-trait associations that surpassed prespecified statistical significance. A *P* of 0.05 / 13 = 0.004 was set for statistical significance for these restricted analyses.

Association for single genic homozygotes. We performed an exploratory analysis of gene-trait pairs where there was only one phenotyped homozygous null. We performed the above association analyses for genes where there was only one homozygous null phenotyped for a given trait and we focused on those with the most extreme standard Z score statistics (|Z score| > 5) from the primary association analysis and required that there to also be nominal evidence for association ($P < 0.05$) in heterozygotes as well to maximize confidence in an observed single homozygous null-trait association.

Methods for recruitment and phenotyping of an *APOC3* p.Arg19Ter proband and relatives.

Methods for Sanger sequencing. We collected blood samples from a total of 28 subjects, including one of the four *APOC3* p.Arg19Ter homozygous participants along with 27 of his family and community members for DNA extraction and separated into plasma for lipid and apolipoprotein measurements. All subjects were consented prior to initiation of the studies (IRB: 00007048 at the Center for Non-Communicable Diseases, Paksitan). DNA was isolated from whole blood using a reference phenol-chloroform protocol.[38] Genotypes for the p.Arg19Ter variant were determined in all 28 participants

by Sanger sequencing. A 685 bp region of the *APOC3* gene including the base position for this variant was amplified by PCR (Expand HF PCR Kit, Roche) using the following primer sequences: Forward primer CTCCTTCTGGCAGACCCAGCTAAGG, Reverse primer CCTAGGACTGCTCCGGGGAGAAAG. PCR products were purified with Exo-SAP-IT (Affymetrix) and sequenced via Sanger sequencing using the same primers.

Oral fat tolerance test. Six non-carriers and seven homozygotes also participated in an oral fat tolerance test. Participants fasted overnight and then blood was drawn for measurement of baseline fasted lipids. Following this, participants were administered an oral load of heavy cream (50 g fat per square meter of body surface area as calculated by the method of Mosteller[39]). Participants consumed this oral load within a time span of 20 minutes and afterwards consumed 200 mL of water. Blood was drawn at 2, 4, and 6 hours after oral fat consumption as done previously.[40,41] All lipid and apolipoprotein measurements from these plasma samples were determined by immunoturbidimetric assays on an ACE Axcel Chemistry analyzer (Alfa Wasserman). A comparisons of area-under-the curve triglycerides was performed between *APOC3* p.Arg19Ter homozygotes and non-carriers using a two independent sample Student's t test; $P < 0.05$ was considered statistically significant.

549 **Tables**

550 **Table 1. Baseline characteristics of exome sequenced study participants.**

Characteristic	Value (n = 7,078)
Age (yrs) – mean (sd)	50.7 (9.1)
Women – no. (%)	1,249 (17.6 %)
Parents closely related – no. (%)	2,710 (38.3 %)
Spouse closely related – no. (%)	2,697 (38.1 %)
Ethnicity – no. (%)	
Urdu	2,647 (37.4 %)
Punjabi	2,332 (32.9 %)
Sindhi	797 (11.3 %)
Pathan	416 (5.9 %)
Memon	108 (1.5 %)
Gujrati	89 (1.3 %)
Balochi	85 (1.2 %)
Other	604 (8.5 %)
Hypertension – no. (%)[*]	3,936 (55.6 %)
Hypercholesterolemia – no. (%)[†]	1,857 (26.2 %)
Diabetes mellitus – no. (%)[‡]	2,904 (41.0 %)
Coronary heart disease – no. (%)[§]	3,046 (43.0 %)
Smoking – no. (%)[‖]	2,814 (39.8 %)

BMI (m/kg^2) – mean (sd)	25.9 (4.3)

[*]Hypertension defined as systolic blood pressure ≥140 mmHg, diastolic blood pressure ≥90 mmHg, or antihypertensive treatment.

[†]Hypercholesterolemia defined as serum total cholesterol >240 mg/dL, lipid lowering therapy or self-report.

[‡]Diabetes defined as fasting blood glucose ≥126 mg/dL, or HbA1c >6.5 %, oral hypoglycemics, insulin treatment, or self-report.

[§]Coronary heart disease defined as history of myocardial infarction as determined by clinical symptoms with typical EKG findings or elevated serum troponin I.

[‖]Smoking defined as active current or prior tobacco smoking.

561 **Figure Legends**

562 **Fig 1.** Consanguinity leads to regions of genomic segments that are identical by descent
563 and can be observed as runs of homozygosity. Using genome-wide array data in 17,744
564 PROMIS participants and reference samples from the International HapMap 3, the
565 burden of runs of homozygosity (minimum 1.5 Mb) per individual was derived and
566 population-specific distributions are displayed, with outliers removed. This highlights the
567 higher median runs of homozygosity burden in PROMIS and the higher proportion of
568 individuals with very high burdens.

569

570 **Fig 2.** The site-frequency spectrum of synonymous, missense, and high-confidence null
571 mutations is represented. Points represent the proportion of variants within a 1×10^{-4}
572 minor allele frequency bin for each variant category. Lines represent the cumulative
573 proportions of variants categories. The bottom inset highlights that most null variants are
574 often seen in no more than one or two individuals. The top inset highlights that virtually
575 all null mutations are very rare.

576

577 **Fig 3. a**, The distribution of F inbreeding coefficient of PROMIS participants is
578 compared to those of outbred samples of African (AFR) and European (EUR) ancestry.
579 **b**, The burden of homozygous null genes per individual is correlated with coefficient of
580 inbreeding.

581

582 **Fig 4. a.-d.** Among all sequenced participants, apolipoprotein C-III, triglycerides, HDL
583 cholesterol and LDL cholesterol distributions are displayed by *APOC3* null genotype

584 status. Apolipoprotein C-III concentration is displayed on a logarithmic base 10 scale. **e.**
585 One of the four *APOC3* null homozygotes and several family members were recruited for
586 genotyping *APOC3* p.Arg19Ter. The proband was married to another null homozygote
587 and has nine obligate homozygote children. Given the extensive first-degree unions, the
588 pedigree is simplified for clarity. **f.** *APOC3* p.Arg19Ter homozygotes and non-carriers
589 within the recruited family participated in an oral 50 g/m^2 fat tolerance test. Homozygotes
590 had decreased baseline and post-prandial triglyceride concentrations.
591
592 **Fig 5.** The anticipated number of unique homozygous null genes observed with
593 increasing sample sizes sequenced in PROMIS compared with similar African (AFR) and
594 European (EUR) sample sizes using observed allele frequencies and degree of
595 inbreeding.

596 **Figures**

597

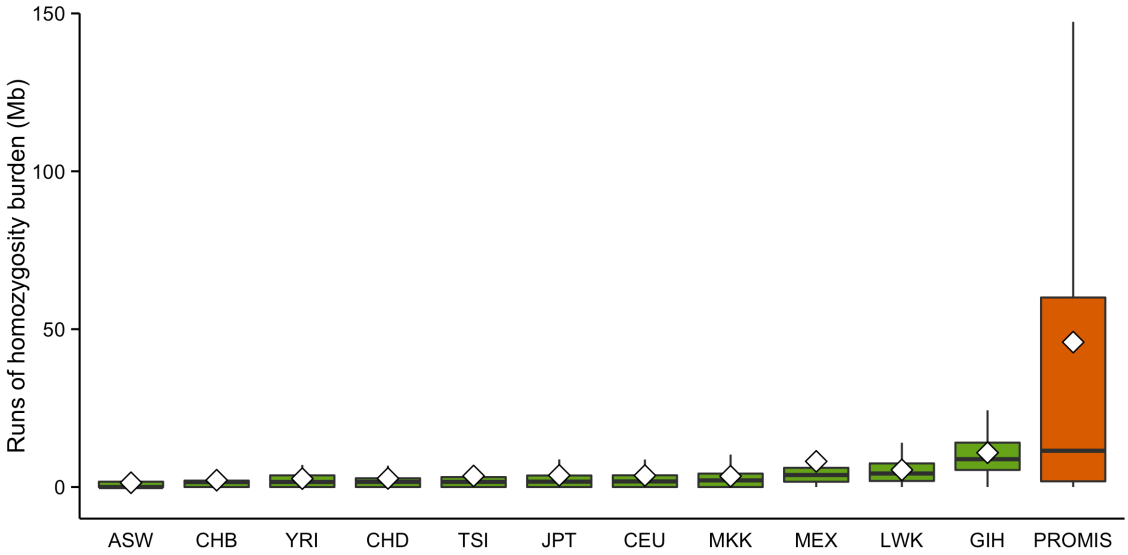

598

599 **Fig 1. PROMIS participants have an excess burden of runs of homozygosity**

600 **compared with other populations.**

601

602

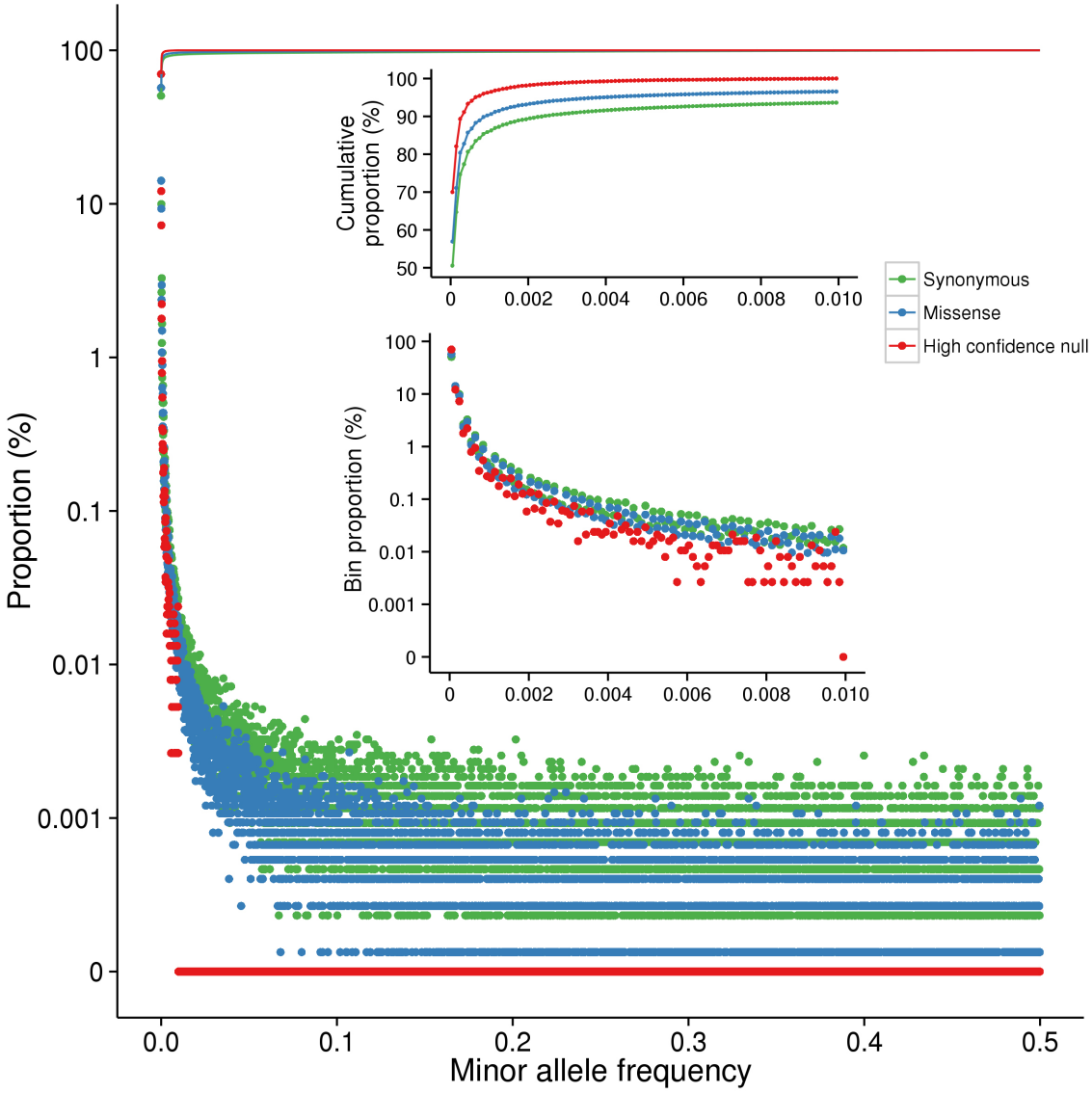

603

604 **Fig 2. Null mutations are typically seen in very few individuals.**

605

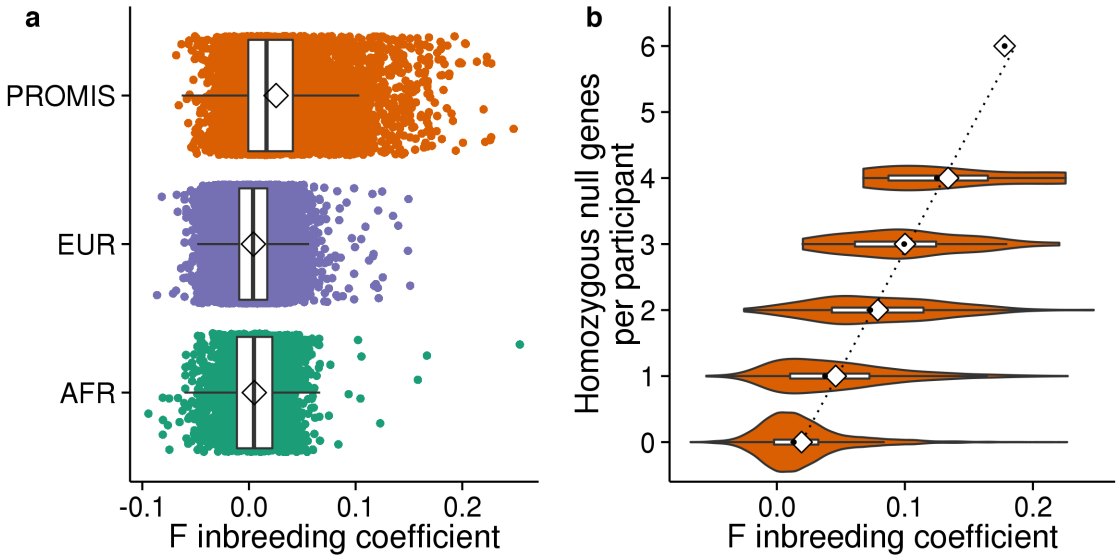

606

607 **Fig. 3. Homozygous null burden in PROMIS is driven by excess autozygosity.**

608

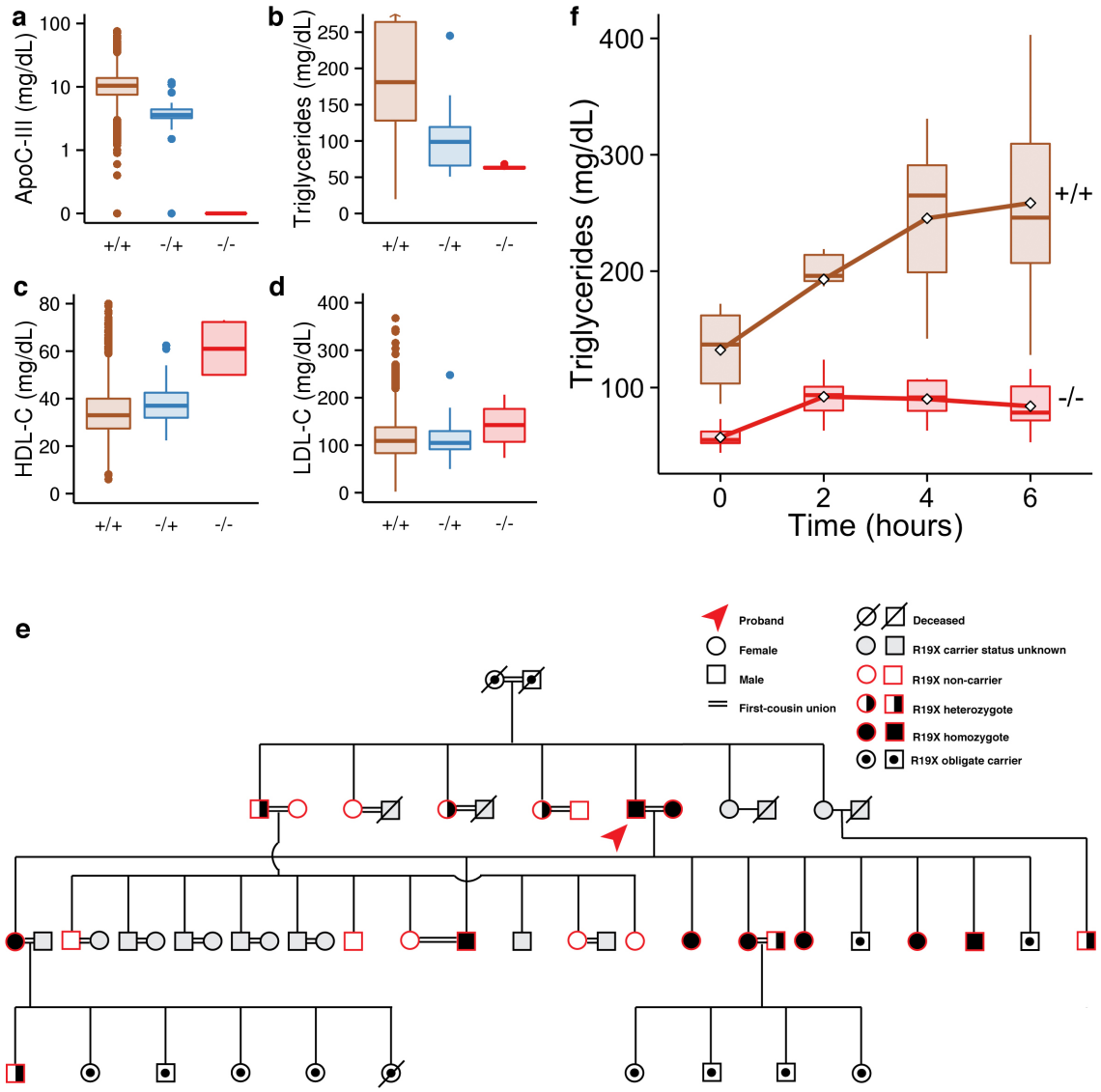

609

610

611 **Fig 4. *APOC3* null homozygotes have diminished fasting triglycerides and blunted**

612 **post-prandial lipemia.**

613

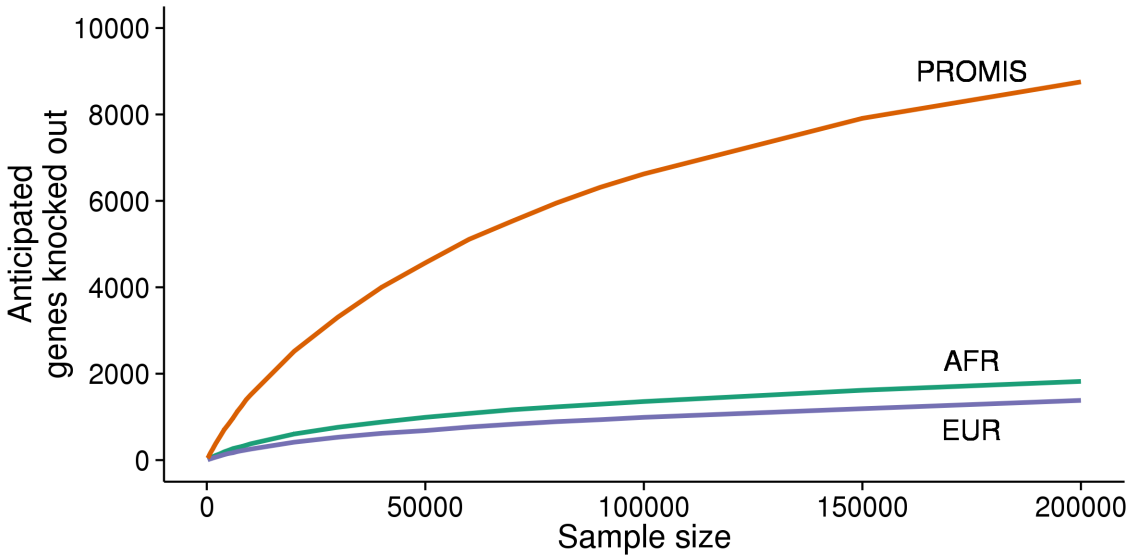

614

615 **Fig 5. Simulations anticipate many more homozygous null genes in the PROMIS**

616 **cohort.**

References

1 Eisenberg, D., Marcotte, E. M., Xenarios, I. & Yeates, T. O. Protein function in the post-genomic era. *Nature* **405**, 823-826, doi:10.1038/35015694 (2000).

2 MacArthur, D. G. *et al.* A systematic survey of loss-of-function variants in human protein-coding genes. *Science* **335**, 823-828, doi:10.1126/science.1215040 (2012).

3 Sulem, P. *et al.* Identification of a large set of rare complete human knockouts. *Nat Genet*, doi:10.1038/ng.3243 (2015).

4 Bittles, A. H., Mason, W. M., Greene, J. & Rao, N. A. Reproductive behavior and health in consanguineous marriages. *Science* **252**, 789-794 (1991).

5 Saleheen, D. *et al.* The Pakistan Risk of Myocardial Infarction Study: a resource for the study of genetic, lifestyle and other determinants of myocardial infarction in South Asia. *European Journal of Epidemiology* **24**, 329-338, doi:10.1007/s10654-009-9334-y (2009).

6 Modell, B. & Darr, A. Science and society: genetic counselling and customary consanguineous marriage. *Nat Rev Genet* **3**, 225-229, doi:10.1038/nrg754 (2002).

7 Lander, E. S. & Botstein, D. Homozygosity mapping: a way to map human recessive traits with the DNA of inbred children. *Science* **236**, 1567-1570 (1987).

8 Karczewski, K. J. *LOFTEE (Loss-Of-Function Transcript Effect Estimator)*, <https://github.com/konradjk/loftee> (2015).

9 De Rubeis, S. *et al.* Synaptic, transcriptional and chromatin genes disrupted in autism. *Nature* **515**, 209-215, doi:10.1038/nature13772 (2014).

10 Samocha, K. E. *et al.* A framework for the interpretation of de novo mutation in human disease. *Nat Genet* **46**, 944-950, doi:10.1038/ng.3050 (2014).

11 Finn, A. V., Nakano, M., Narula, J., Kolodgie, F. D. & Virmani, R. Concept of vulnerable/unstable plaque. *Arterioscler Thromb Vasc Biol* **30**, 1282-1292, doi:10.1161/ATVBAHA.108.179739 (2010).

12 Carr, B. A., Wan, J., Hines, R. N. & Yost, G. S. Characterization of the human lung CYP2F1 gene and identification of a novel lung-specific binding motif. *The Journal of Biological Chemistry* **278**, 15473-15483, doi:10.1074/jbc.M300319200 (2003).

13 Standiford, T. J. *et al.* Interleukin-8 gene expression by a pulmonary epithelial cell line. A model for cytokine networks in the lung. *The Journal of Clinical Investigation* **86**, 1945-1953, doi:10.1172/JCI114928 (1990).

14 Christiansen, D. *et al.* Humans lack iGb3 due to the absence of functional iGb3-synthase: implications for NKT cell development and transplantation. *PLoS Biology* **6**, e172, doi:10.1371/journal.pbio.0060172 (2008).

15 Dahl, K., Buschard, K., Gram, D. X., d'Apice, A. J. & Hansen, A. K. Glucose intolerance in a xenotransplantation model: studies in alpha-gal knockout mice. *APMIS : Acta Pathologica, Microbiologica, et Immunologica Scandinavica* **114**, 805-811, doi:10.1111/j.1600-0463.2006.apm_393.x (2006).

16 Casu, A. *et al.* Insulin secretion and glucose metabolism in alpha 1,3-galactosyltransferase knock-out pigs compared to wild-type pigs. *Xenotransplantation* **17**, 131-139, doi:10.1111/j.1399-3089.2010.00572.x (2010).

17 Schneider, M. R. & Wolf, E. The epidermal growth factor receptor ligands at a glance. *Journal of Cellular Physiology* **218**, 460-466, doi:10.1002/jcp.21635 (2009).

18 Wang, G. X. *et al.* The brown fat-enriched secreted factor Nrg4 preserves metabolic homeostasis through attenuation of hepatic lipogenesis. *Nature Medicine* **20**, 1436-1443, doi:10.1038/nm.3713 (2014).

19 Huff, M. W. & Hegele, R. A. Apolipoprotein C-III: going back to the future for a lipid drug target. *Circ Res* **112**, 1405-1408, doi:10.1161/CIRCRESAHA.113.301464 (2013).

20 Tg *et al.* Loss-of-function mutations in APOC3, triglycerides, and coronary disease. *N Engl J Med* **371**, 22-31, doi:10.1056/NEJMoa1307095 (2014).

21 Jorgensen, A. B., Frikke-Schmidt, R., Nordestgaard, B. G. & Tybjaerg-Hansen, A. Loss-of-function mutations in APOC3 and risk of ischemic vascular disease. *N Engl J Med* **371**, 32-41, doi:10.1056/NEJMoa1308027 (2014).

22 Kooner, J. S. *et al.* Genome-wide association study in individuals of South Asian ancestry identifies six new type 2 diabetes susceptibility loci. *Nat Genet* **43**, 984-989, doi:10.1038/ng.921 (2011).

23 Purcell, S. *et al.* PLINK: a tool set for whole-genome association and population-based linkage analyses. *American Journal of Human Genetics* **81**, 559-575, doi:10.1086/519795 (2007).

24 Tennessen, J. A. *et al.* Evolution and functional impact of rare coding variation from deep sequencing of human exomes. *Science* **337**, 64-69, doi:10.1126/science.1219240 (2012).

25 Do, R. *et al.* Exome sequencing identifies rare LDLR and APOA5 alleles conferring risk for myocardial infarction. *Nature*, doi:10.1038/nature13917 (2014).

686 26 Fisher, S. *et al.* A scalable, fully automated process for construction of sequence-
687 ready human exome targeted capture libraries. *Genome Biology* **12**, R1,
688 doi:10.1186/gb-2011-12-1-r1 (2011).
689 27 Li, H. & Durbin, R. Fast and accurate short read alignment with Burrows-Wheeler
690 transform. *Bioinformatics* **25**, 1754-1760, doi:10.1093/bioinformatics/btp324
691 (2009).
692 28 McKenna, A. *et al.* The Genome Analysis Toolkit: a MapReduce framework for
693 analyzing next-generation DNA sequencing data. *Genome Research* **20**, 1297-
694 1303, doi:10.1101/gr.107524.110 (2010).
695 29 DePristo, M. A. *et al.* A framework for variation discovery and genotyping using
696 next-generation DNA sequencing data. *Nat Genet* **43**, 491-498,
697 doi:10.1038/ng.806 (2011).
698 30 Van der Auwera, G. A. *et al.* From FastQ data to high confidence variant calls:
699 the Genome Analysis Toolkit best practices pipeline. *Current Protocols in*
700 *Bioinformatics* **11**, 11 10 11-11 10 33, doi:10.1002/0471250953.bi1110s43
701 (2013).
702 31 McLaren, W. *et al.* Deriving the consequences of genomic variants with the
703 Ensembl API and SNP Effect Predictor. *Bioinformatics* **26**, 2069-2070,
704 doi:10.1093/bioinformatics/btq330 (2010).
705 32 Jun, G. *et al.* Detecting and estimating contamination of human DNA samples in
706 sequencing and array-based genotype data. *American Journal of Human Genetics*
707 **91**, 839-848, doi:10.1016/j.ajhg.2012.09.004 (2012).

33 Manichaikul, A. *et al.* Robust relationship inference in genome-wide association studies. *Bioinformatics* **26**, 2867-2873, doi:10.1093/bioinformatics/btq559 (2010).

34 Hunter-Zinck, H. *et al.* Population genetic structure of the people of Qatar. *American Journal of Human Genetics* **87**, 17-25, doi:10.1016/j.ajhg.2010.05.018 (2010).

35 Purcell, S. M. *et al.* A polygenic burden of rare disruptive mutations in schizophrenia. *Nature* **506**, 185-190, doi:10.1038/nature12975 (2014).

36 Wright, S. Coefficients of inbreeding and relationship. *Am Nat* **56**, 330-338 (1922).

37 Price, A. L. *et al.* Principal components analysis corrects for stratification in genome-wide association studies. *Nat Genet* **38**, 904-909, doi:10.1038/ng1847 (2006).

38 Sambrook, J. & Russell, D. W. Purification of nucleic acids by extraction with phenol:chloroform. *CSH protocols* **2006**, doi:10.1101/pdb.prot4455 (2006).

39 Mosteller, R. D. Simplified calculation of body-surface area. *N Engl J Med* **317**, 1098, doi:10.1056/NEJM198710223171717 (1987).

40 Maraki, M. *et al.* Validity of abbreviated oral fat tolerance tests for assessing postprandial lipemia. *Clinical Nutrition* **30**, 852-857, doi:10.1016/j.clnu.2011.05.003 (2011).

41 Pollin, T. I. *et al.* A null mutation in human APOC3 confers a favorable plasma lipid profile and apparent cardioprotection. *Science* **322**, 1702-1705, doi:10.1126/science.1161524 (2008).

731 **Supplementary Information** is linked to the online version of the paper at

732 www.nature.com/nature.

733

734 **Acknowledgements** Dr. Saleheen is supported by grants from the National Institutes of
735 Health, the Fogarty International, the Wellcome Trust, the British Heart Foundation, and
736 Pfizer. Dr. Natarajan is supported by the John S. LaDue Memorial Fellowship in
737 Cardiology from Harvard Medical School. Dr. Kathiresan is supported by grants from the
738 National Institutes of Health (R01HL107816), the Donovan Family Foundation, and
739 Fondation Leducq. Exome sequencing was supported by a grant from the NHGRI
740 (5U54HG003067-11) to Drs. Gabriel and Lander. Dr. MacArthur is supported by a grant
741 from the National Institutes of Health (R01GM104371). In recognition for PROMIS
742 fieldwork and support, we also acknowledge contributions made by the following:
743 Mohammad Zeeshan Ozair, Usman Ahmed, Abdul Hakeem, Hamza Khalid, Kamran
744 Shahid, Fahad Shuja, Ali Kazmi, Mustafa Qadir Hameed, Naeem Khan, Sadiq Khan,
745 Ayaz Ali, Madad Ali, Saeed Ahmed, Muhammad Waqar Khan, Muhammad Razaq Khan,
746 Abdul Ghafoor, Mir Alam, Riazuddin, Muhammad Irshad Javed, Abdul Ghaffar, Tanveer
747 Baig Mirza, Muhammad Shahid, Jabir Furqan, Muhammad Iqbal Abbasi, Tanveer Abbas,
748 Rana Zulfiqar, Muhammad Wajid, Irfan Ali, Muhammad Ikhlaq, Danish Sheikh,
749 Muhammad Imran, Matthew Walker, Nadeem Sarwar, Sarah Venorman, Robin Young,
750 Adam Butterworth, Hannah Lombardi, Binder Kaur and Nasir Sheikh. Fieldwork in the
751 PROMIS study has been supported through funds available to investigators at the Center
752 for Non-Communicable Diseases, Pakistan and the University of Cambridge, UK.

753

754

755 **Author Contributions** Sample recruitment and phenotyping was performed by D.S.,
756 P.F., J.D., A.R., M.Z., M.S., M.F., A.I., N.K.S., S.A., F.M., M.I., S.A., K.T., N.H.M.,
757 K.S.Z., N.Q., M.I., S.Z.R., F.M., K.M., and N.A.. D.S., P.F., J.D., and W.Z. performed
758 array-based genotyping and runs-of-homozygosity analyses. Exome sequencing was
759 coordinated by D.S., N.G., S.G., E.S.L., D.J.R., and S.K.. P.N., W.Z., H.H.W., and R.D.
760 performed exome sequencing quality control and association analyses. P.N., K.J.K.,
761 A.H.O., and D.G.M. performed variant annotation. D.S., S.K. and D.J.R. performed
762 confirmatory genotyping and lipoprotein biomarker assays. D.S. and A.R. conducted
763 recall based studies for the APOC3 knockouts. P.N. and M.J.D. performed bioinformatics
764 simulations. P.N. and K.E.S. performed constraint score analyses. D.S., P.N., and S.K.
765 designed the study and wrote the paper. D.S. and P.N. contributed equally. All authors
766 discussed the results and commented on the manuscript.

767

768 **Author Information** Summaries of all null variants observed in a homozygous are in the
769 online Supplement. They are additionally, with all observed protein-coding variation,
770 publicly available in the Exome Aggregation Consortium browser
771 (exac.broadinstitute.org). Reprints and permissions information is available at
772 www.nature.com/reprints. The authors do not declare competing financial interests.
773 Correspondence and requests for materials should be addressed to D.S. or S.K.
774 (saleheen@mail.med.upenn.edu or sekar@broadinstitute.org).